COMPUTER ANALYSIS OF ORGANELLE TRANSLOCATION IN PRIMARY NEURONAL CULTURES AND CONTINUOUS CELL LINES

ANTHONY C. BREUER, CLIFFORD N. CHRISTIAN, MARYANNA HENKART, and PHILLIP G. NELSON

From the Behavioral Biology Branch, National Institute of Child Health and Human Development, National Institutes of Health, Bethesda, Maryland 20014. Dr. Breuer's present address is Department of Neurology, Childrens Hospital Medical Center, Boston, Massachusetts 02115.

ABSTRACT

Organelle translocation in a number of cell types in tissue culture as seen by high-resolution Zeiss-Nomarski differential interference contrast optics was filmed and analyzed by computer. Principal cell types studied included primary chick spinal cord, chick dorsal root ganglion, rat brain, and various clones of continuous cell lines. Organelle translocations in all cell types studied exhibited frequent, large changes in velocity during any one translocation. The appearance of particles as seen with Nomarski optics was correlated with their fine structures in one dorsal root ganglion neurite by fixing the cell as it was being filmed and obtaining electron micrographs of the region filmed. This revealed the identity of several organelles as well as the presence of abundant neurotubules but no neurofilaments. Primary cell cultures exhibited more high-velocity organelle movements than continuous cell lines. The net progress of an organelle in a given direction was greater in primary neuronal cells than in fibroblasts or continuous cell lines. These findings are correlated with the literature on organelle translocation and axoplasmic transport.

The literature on axoplasmic transport is composed chiefly of findings made with indirect methods of measuring the rate of displacement of axoplasmic components. Such methods have included the measurement of transport of radioactive isotopes (19, 20, 25) or of specific cytochemical markers (7, 22). While cytoplasmic streaming, motility, and saltatory particle motion in a number of non-neuronal cell systems have been extensively studied (28), microscopic analysis of particle or organelle transport in vertebrate neuronal tissues has been the subject of relatively few reports. Even more scarce are studies on this type of transport in dissociated neurons in tissue culture. The purpose of this report is to provide quantitative data on organelle transport in several types of vertebrate neurons in tissue culture and to relate these data to current hypotheses of organelle translocation. Cultured cell types studied included chick embryo spinal cord, chick embryo dorsal root ganglion (DRG) cells, rat embryo brain cells, various clones of neuroblastoma, L cells, HeLa cells, and mouse embryo fibroblasts.

MATERIALS AND METHODS

Cell Cultures

All cultures were grown on round 25-mm diameter no. 1½ Corning no. 2910 lead oxide-free cover glasses in 35-mm Falcon (Falcon Plastics, Div. of Bioquest, Ox-

nard, Calif.) or Lux (Lux Scientific Corp., Thousand Oaks, Calif.) polystyrene dishes. Except in the case of the HeLa cells, L cells, and several neuroblastoma clones examined, the cover glasses were pretreated with a layer of clear MS-122 fluorocarbon spray (Miller-Stephenson Chemical Co. Inc., Danbury, Conn.) and subsequently with 3–4 drops of rat tail collagen solution prepared following the method of Bornstein (4) but not dialyzed. Collagen was dried down onto the cover glasses overnight in a 40°C oven to insure that cells would not subsequently peel off as a mat from the glass surface.

Spinal cord cells from whole cords of 7-day old White Leghorn Arbor Acre no. 26 chick embryos (Truslow Farms, Chestertown, Md.) were dissected, dissociated in 0.25% trypsin (Microbiological Associates, Bethesda, Md.), and maintained following the method of Fischbach (11) in Eagle's minimal essential medium (MEM) supplemented with 10% horse serum (HS) (Microbiological Associates) and 10% chick embryo extract (CEE). No cytotoxic agents were used to eliminate dividing cells. Some spinal cord cultures were plated on top of chick pectoral muscle which had been cultured for 5 days, a procedure which seemed to enhance the maturation and survival of spinal cord cells. Pectoral muscle was prepared and grown by techniques described (11) and was plated at 150,000 cells per 35-mm dish in 1.5 cm^3 of medium. Spinal cord cells were plated at 100,000 cells per dish. Media for these and other cell types described below were changed three times a week.

DRG were dissected from 9–11-day old chick embryos, dissociated in trypsin, and grown either with or without nerve growth factor (NGF) (kindly provided by Dr. H. Ronald Fisk) at concentrations of 0.2 μg/ml, in Eagle's MEM supplemented with 10% HS and 10% CEE. As previously documented (21), NGF was observed to improve survival of dissociated DRG cells.

Mechanically dissociated rat brain cells from 15-day old embryos were grown in Dulbecco's modified Eagle's MEM (DMEM) supplemented with 10% fetal calf serum (FCS) (Colorado Serum Co., Denver, Colo.) by the method of Godfrey et al.[1] Such cells could be maintained for periods of 30 days or more.

Neuroblastoma clone N18 was grown in DMEM with 10% FCS, and clones SB27B and NX31 were grown in this medium supplemented with 1×10^{-4} M hypoxanthine, 1×10^{-5} M aminopterin (American Cyanamid Co., Lederle Laboratories Div., Pearl River, N. Y.), 1.6×10^{-5} M thymidine (HAT). Cells were plated at a density of 20,000 cells per dish. Removal of FCS from the medium of N18 promoted the formation of processes (29), which were studied 1–3 days after serum removal. 3 days after plating, clone NX31 was treated with 1 mM dibutyryl cyclic 3',5'-adenosine monophosphate (db-cAMP) and examined a day later. Clone SB27B was inspected 1 day after plating or 15 days after treatment with 4×10^{-7} M aminopterin. Fibroblasts studied were those seen in primary cultures of dissociated mouse DRG cells grown in DMEM supplemented with 10% FCS and 0.1 μg/ml NGF.

Strain LM (TK^-) L cells, an established cell line of mouse fibroblastic origin, were grown in DMEM supplemented with 10% FCS (24). On attaining confluent growth, the cultures received 5,000 rad of X-irradiation, were resuspended 3 days later in 0.25% trypsin solution, and replated. They were treated with 1 mM db-cAMP after another 3 days. Highly processed cells were thus obtained within 6 h and examined for organelle translocation.

HeLa cells, strain R (Grand Island Biological Co., Grand Island, N. Y.) were grown in Eagle's MEM supplemented with 1× nonessential amino acids and 10% calf serum (Flow Laboratories, Rockville, Md.). Treatment of these cells with 5 mM Na butyrate promoted the formation of processes (15) which were examined for organelle translocation.

Cinemicrography

A cover glass with attached cells was mounted in a Dvorak-Stotler controlled environment culture chamber (8) and examined under Zeiss-Nomarski differential interference contrast optics utilizing the oil immersed planapochromat 100/1.25 objective and immersed achromat aplanat 1.4 condensor of a Carl Zeiss Photomicroscope II. Compensator settings were adjusted to permit 0.5-s exposures on 4×-reversal 16-mm film using a DC powered HBO 200/W4 arc. Exposures were taken at a framing rate of one per second on a Bolex 5 DTBC-M5 camera equipped with time-lapse drive (Industrial Camera Co., Epsom, N. H.). The constancy of the 1-s intervals was monitored by three-place digital readout of timing relay output. A Zeiss VG9 green filter and BG38 heat filter were used throughout. The 5,000 feet of film taken were commercially spray processed using a modified reversal formula (Byron Motion Pictures, Washington, D. C.). The numbers of cover glass cultures filmed and the total number of separate dissections or platings studied are summarized in Table I.

Temperature Experiments

A C-300 Air Stream Stage incubator (Nicholson Precision Instruments, Bethesda, Md.) with proportional thermistor feedback control was used to direct a current of warm air onto the top surface of the culture chamber. The output of a YSI 421 thermistor probe (Yellow Springs Instrument Company, Inc., Yellow Springs, Ohio) affixed with Dow heat sink compound to the pressure plate of the chamber was read on a YSI tele-thermometer (model 44TA) and recorded via a Brush 280 recorder (Gould, Inc., Cleveland, Ohio). Recordings from this thermistor were calibrated against those simultaneously obtained from another YSI 421

[1] Godfrey, E. W., P. G. Nelson, B. K. Schrier, A. C. Breuer, and B. R. Ransom. Manuscript submitted for publication.

TABLE I

Summary of Numbers of Cultures of Primary Neuronal and Continuous Cell Lines in Which Organelle Translocation was Filmed

Cell type	Total no. dissections or platings	Total no. cover glass cultures filmed
Chick embryo spinal cord	5	17
Chick embryo DRG	9	15
Rat embryo brain	3	5
Neuroblastoma clones	5	6
Mouse embryo DRG fibroblasts	1	1
Rat embryo brain fibroblasts	1	1
L cells	1	2
HeLa cells	1	2

thermistor probe seated in a precisely drilled hole in the top cover glass of the chamber (kindly loaned by Dr. J. A. Dvorak) in such a fashion that its temperature-sensitive surface was coplanar with the undersurface of the top cover glass. Simultaneous recordings from both thermistors were repeated eight times over 2 days, increasing the temperature of the chamber in several-degree increments over the range 29°-38°C at 5-min intervals during each trial. The resulting curves from the eight calibration runs were virtually superimposable, with the pressure plate thermistor recording 1.3° ± 0.1°C lower than the cover glass thermistor at all temperatures. Thus, during filming the temperature of the undersurface of the top cover glass, where the cells were located, could be accurately determined. During temperature experiments, organelle translocation was filmed only during the last 2 min of the 5-min interval at any temperature setting. During these last 2 min, the change in temperature of the undersurface of the cover glass was minimal (±0.1°C). For other experiments the temperature of the undersurface of the top cover glass was maintained at 36.4° ± 0.1°C.

pH Experiments

The short-term effect of environmental pH changes on organelle translocation was determined by perfusing in turn into the chamber Earle's balanced salt solution with a pH of 5.3, 6.3, 7.4, 8.1, and 9.0. The chamber volume, 0.25 ml, was exchanged eight times with each perfusate and the cells were subsequently filmed in their new pH environment for 5 min.

Variation with Time and Cell Cluster to Cell Cluster Variability

The variability of organelle transport with time in our system was estimated by filming several cell clusters for 66 min. In addition, several active cell clusters were filmed for 10-min intervals to evaluate cluster to cluster variability in organelle velocities or behavior.

Ultrastructural Studies

Two cultures of dissociated DRG cells were fixed by perfusion of the chamber with 2.5% glutaraldehyde in 0.15 M cacodylate buffer, pH 7.4, while filming continued. Actively moving organelles were found to be motionless within the time taken to refocus the microscope image (at most, 9 s) after alteration of focus due to perfusion. 35-mm light micrographs (100× objective, Nomarski optics) taken before and after fixation were virtually indistinguishable, demonstrating no shrinkage or distortion of cells.

The cultures were postfixed in osmium tetroxide, block stained in uranyl acetate, dehydrated in ethanol, and embedded in Epon. After polymerization of the plastic, the cover glass was removed and the previously filmed neurite relocated under phase optics. The area of interest was then marked using a needle held in a micromanipulator, cut out, mounted, and serial sections parallel to the plane of the cover glass were made. Sections were stained with uranyl acetate and lead citrate.

Analysis of Data

Processed film was projected via an L-W Photo-Optical Data Analyser model 224 A (L-W Photo Inc., Van Nuys, Calif.) onto a Moseley Autograph X-Y Recorder model 2 DR-2AM (F. L. Moseley Co., Pasadena, Calif.). Two analogue voltages simultaneously drove the pen of the X-Y recorder, and the A/D converters of a PDP-12 computer (Digital Equipment Corp., Maynard, Mass.) producing digitized frame-by-frame coordinates for each particle. Organelles tracked were those that remained in focus and clearly distinguishable from other organelles and structures for at least several frames. The thickness of a cell process or neurite bundle could therefore influence the results to some extent by providing a greater or lesser opportunity for an organelle to leave the focal plane. Maximum error of identification of organelle location on the projected image was estimated at 0.2 μm. Computer output was graphed by a Digital Plotting Systems Complot (Houston Instrument Div., Bellaire, Tex). Continuous cell lines had neurites which could be clearly traced to a soma, and the somatofugal movement of particles was assigned a positive velocity. The direction of movement in other cell types was arbitrarily defined.

Definition of Terms

In order to make more readily understandable the results described below and the subsequent discussion of them, the following terms are defined:

(*a*) A translocation is the continuous motion of a discriminable organelle between resting states. In our system, this criterion yielded translocations of at least 0.2 μm/s over four frames or more. These organelle motions fulfill the criteria for saltations as discussed in detail by Rebhun (28), and are not random Brownian movements.

The term translocation is not intended to imply anything about the mechanism of motion. It is preferred over the term saltation because to describe these organelle motions as "jumps" seems to oversimplify the nature of the movement which is characterized by a series of widely varying velocities during any one "jump."

(*b*) A 1-s velocity of an organelle is defined as the distance a particle moves from one frame to the next when the interval between frames is 1 s. This was the standard framing rate in the present study.

(*c*) The translocation velocity of an individual organelle movement is the total distance traversed during a translocation divided by the total length of time taken to traverse it. This is equivalent to a vector average of all the 1-s velocities manifested during a given translocation.

(*d*) The mean translocation velocity is an average of the translocation velocities of all organelles tracked within a particular cell process or neurite bundle.

(*e*) The vector-scaler ratio (VSR) is an index of the net progress of an organelle in a given direction. It is computed by dividing the vector sum (vector velocity) of all 1-s velocities (where velocities in one direction are subtracted from those in the opposite direction) by the scalar sum (scalar velocity) of all 1-s velocities (where absolute values of velocities are added). Thus, if an organelle were to make a series of translocations all in the same direction, its VSR would be 1.0. If, however, an organelle were to make little net progress in a given direction by reversing its course one or more times, such an organelle would have a VSR considerably less than 1.0. To-and-fro movements producing no net progress result in a VSR of zero.

RESULTS

Primary Neuronal Cultures

MORPHOLOGIC STUDIES: Primary cultures of spinal cord, DRG, and brain cells were studied after 8, 5, and 41 days of age in culture, respectively. Cells were morphologically differentiated at these stages (Figs. 1 *a*, *c*, and 2 *a*). Organelles in each cell type had a similar distribution of sizes and shapes (Figs. 1 *b*, *d*, and 2 *b*) as seen through the light microscope. Round organelles had apparent diameters of 0.3–0.5 μm and elongate organelles had widths ranging from 0.3 to 0.5 μm and lengths of 0.7–1.5 μm.

The detailed correlation of light microscope observations with ultrastructure was done on a DRG cell 1-day in culture. Obvious features distinguishable under high-resolution Nomarski optics in three focal planes were correlated with structures in serial thin sections. Organelles seen in the light micrographs were then identified by locating them on electron micrograph montages at given distances from obvious landmarks such as protrusions from the edge of the neurite.

The process shown in Fig. 3 is a single neurite in which organelle translocation was filmed. The size of organelles as they appeared in electron micrographs of fixed and embedded material was close to the size they appeared to be in Nomarski images. Structures that appeared as particles in Nomarski images included a mitochondrion, a pair of lysosomes, and two cases in which a lysosome adjacent to a multivesicular body appeared as a single particle. Individual lysosomes and multivesicular bodies seen in electron micrographs were not identifiable as particles in our Nomarski photos of this process. Numerous parallel, rather evenly spaced microtubules, and a network of smooth endoplasmic reticulum (ER) were not resolved by the Nomarski system. Tubular elements of ER were 30–60 nm in diameter and often could be traced in parallel with a single microtubule for distances up to 0.5 μm. Membrane-bounded vesicles 80–100 nm in diameter with electron-lucent centers were sometimes arranged in rows parallel to microtubules, and other vesicles of various diameters from 40 to 150 nm with either electron-lucent or -opaque cores and with or without fuzzy coats were scattered along the process. Immediately beneath the surface membrane in scattered areas along the fiber were weblike networks of fine filamentous material, but there were no linearly arranged filaments present among the microtubules. Fibroblasts in the same culture as the filmed DRG contained numerous 60-Å microfilaments and 100-Å filaments, and the same fixation conditions routinely preserve neurofilaments in older cultures of DRG and other neuronal types.

In the region of the neurite just described, organelles were seen moving along the fiber toward and away from the cell body. Four such organelles were documented to traverse the neurite with path lengths of 5–12 μm at translocation velocities of 0.47, 0.33, 0.47, and 0.17 μm/s. One of these moving organelles was located, after fixation, at the point along the process where a lysosome was adjacent to a multivesicular body (Fig. 3 *b*). Whether the lysosome or the multivesicular body was moving or the two were moving together cannot be stated with certainty. However, since individual lysosomes or multivesicular bodies of comparable size in this neurite were not visible as particles in the Nomarski system, it seems likely that the two were moving together.

ORGANELLE MOTION ANALYSIS: Analysis of the translocational activity of organelles in the three types of primary neuronal culture revealed

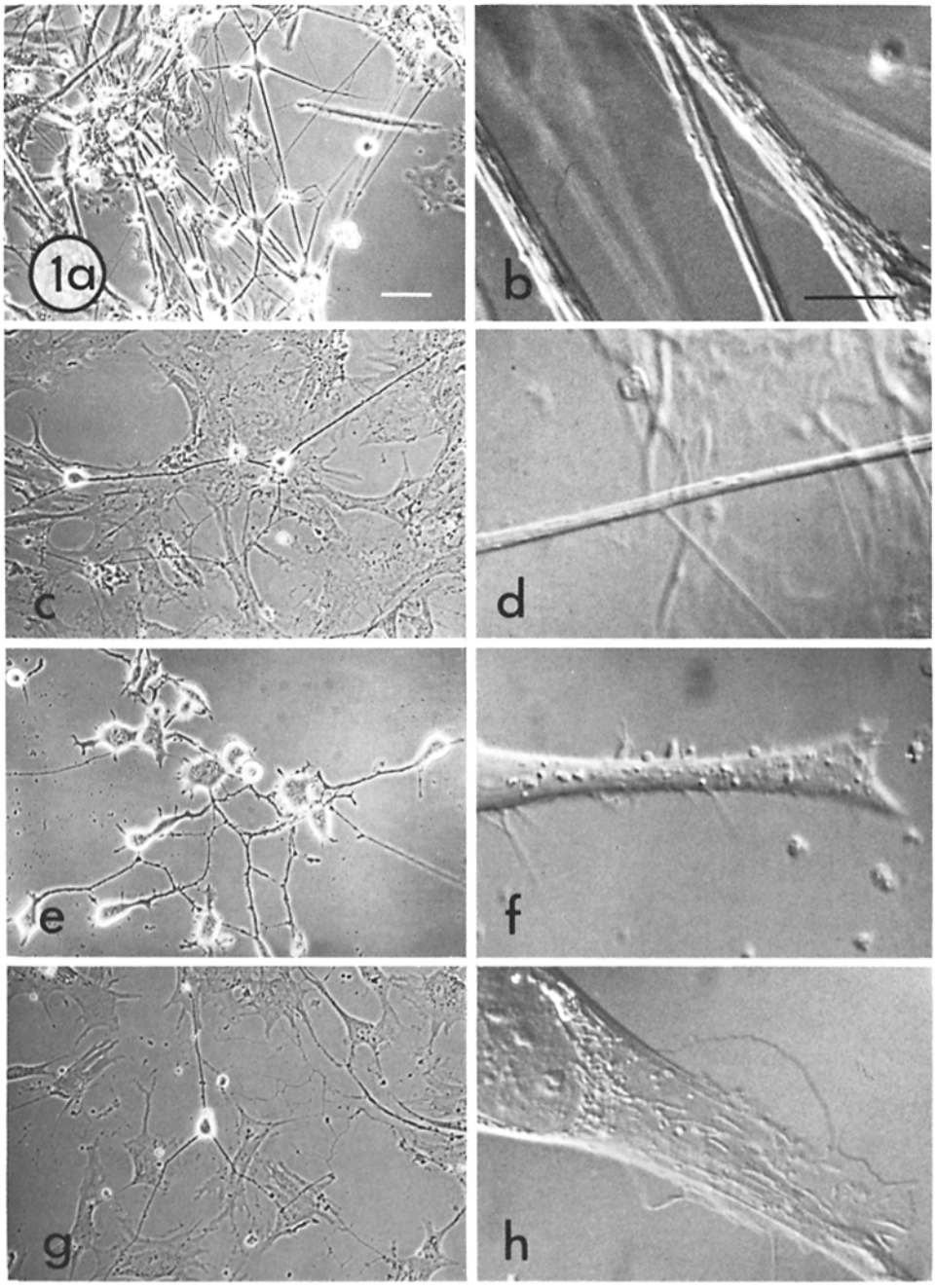

FIGURE 1 Low-power phase-contrast micrographs of cell types analyzed for organelle translocation illustrate the degree of differentiation at the time of analysis of chick embryo spinal cord (*a*), chick embryo DRG (*c*), neuroblastoma clone N18 (*e*), and mouse embryo fibroblasts growing in a culture derived from DRG (*g*). In Fig. 1 *g*, the single phase-bright cell near the center is a DRG neuron. The bar in Fig. 1 *a* indicates 50 μm and applies to Fig. 1 *a*, *c*, *e*, and *g*. To the right of each low-resolution micrograph is a frame from a 16-mm film of organelle transport in that cell type. These frames from analyzed films taken under high-resolution Nomarski differential interference contrast optics illustrate the range of shape and size of organelles at this level of resolution in the cell studied. The bar in Fig. 1 *b* indicates 10 μm and applies to Fig. 1 *b*, *d*, *f*, and *h*.

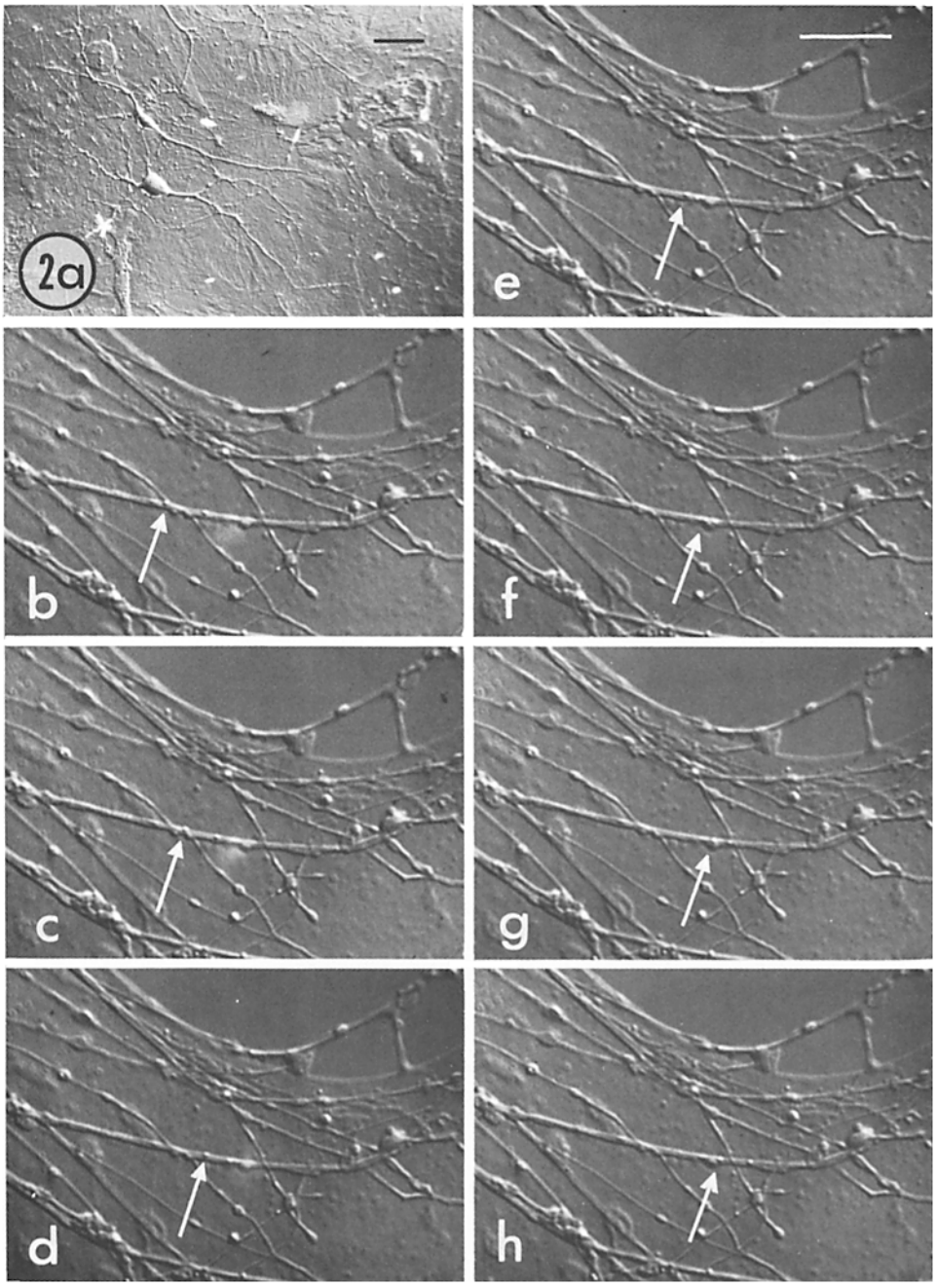

FIGURE 2 Low-resolution Nomarski micrograph (*a*) of rat embryo brain cells 41 days in culture demonstrates the degree of differentiation of these cells at the time they were studied. The bar in Fig. 2 *a* indicates 50 μm. Fig. 2 *b–h* are alternate frames from a segment of 16-mm film taken at one frame per second under higher resolution Nomarski optics. Fig. 2 *h* was thus taken 13 s after Fig. 2 *b*. The progress of organelles across the frame may be traced through the series. The bar in Fig. 2 *e* indicates 10 μm. Thus, the organelle indicated by the arrows moved approximately 9 μm between Fig. 2 *b* and *h*.

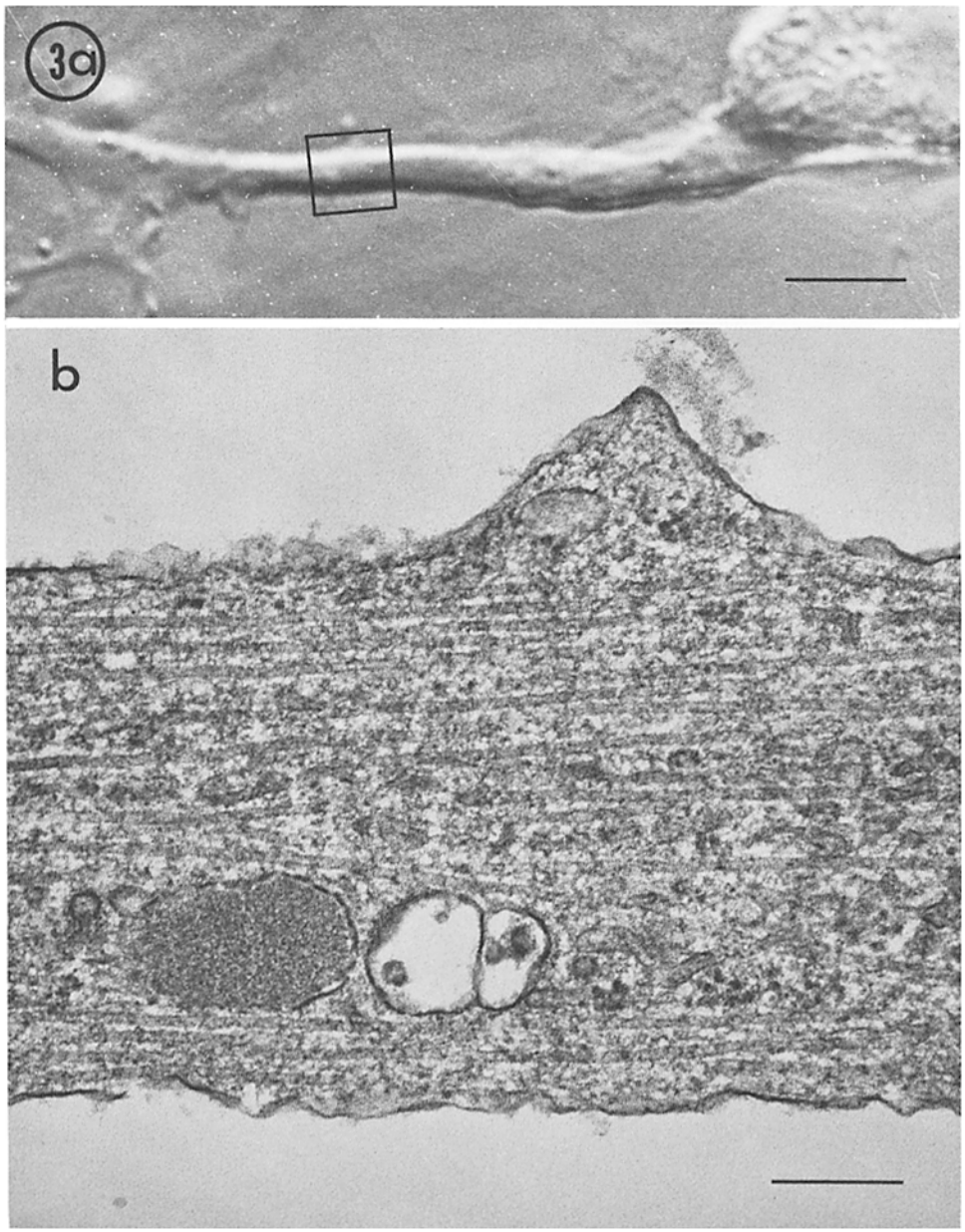

FIGURE 3 The high-resolution Nomarksi micrograph (*a*) is of an isolated chick DRG cell 1 day in culture. A cine film was made of organelles translocating both toward and away from the cell soma, and the cell was then fixed by perfusion of the culture chamber with fixative while filming continued. After being embedded, the cell was relocated under phase-contrast optics, and serial sections were made for ultrastructural analysis. The bar indicates 5 μm. Fig. 3 *b* is an electron micrograph of a thin section through the area enclosed in the box in Fig. 3 *a*. The particle located in this area of the Nomarski micrograph was moving until the moment of fixation. The electron microscope reveals that in this area there was a lysosome adjacent to a multivesicular body. Note the presence of numerous parallel neurotubules and the absence of neurofilaments. The bar indicates 0.25 μm.

that while the translocation velocities of individual organelles varied (Fig. 4, *a*, *c*, *e*), mean translocation velocities of all translocations of all organelles observed in successive 5-min intervals were relatively constant (Fig. 4 *b*, *d*) over the range 0.5–1.25 μm/s throughout the 66-min observation period. Further, this behavior was found not to vary significantly in spinal cord cells over a pH range of 5.3–9.0. The effect of temperature on particle motion was determined by computing the regression line of the average translocational velocity onto temperature, which was increased in four steps from 31.8° to 38.2°C. In three preparations, r equalled 0.192, 0.088 and −0.274, where the number of particles observed was 100, 124, and 32 (not significant at the 0.05 level). The slope of the regression line yielded a Q_{10} of 1.64, 1.19, and 0.67. There was variability among cell clusters, (Table II), and some cells or cell clusters demonstrated no organelle translocation at all.

Frame-by-frame (second-by-second) analyses of individual organelle translocations revealed four additional features of their movement. First, organelle behavior, as seen on the distance vs. time plots (Fig. 5, *a*, *c*, *e*), varied widely in terms of distances traversed after a series of translocations, and number and duration of pauses during movement in one direction. In general, however, organelles in these primary neuronal cultures tended to

TABLE II

Cell Cluster to Cell Cluster Variation in Mean Organelle Translocation Velocities in Dissociated Chick Embryo Spinal Cord Cultures

Cell cluster	No. of translocating organelles analyzed	Mean translocation velocity (μm/s) ± SD
1	10	0.40 ± 0.094
2	4	0.62 ± 0.20
3	4	0.48 ± 0.19
4	3	0.21 ± 0.06
5	20	0.78 ± 0.15
6	47	0.75 ± 0.05

The mean translocation velocity is an average of the translocation velocities as defined in the text (see Materials and Methods) of all organelles tracked within neurite bundles of a given cell cluster.

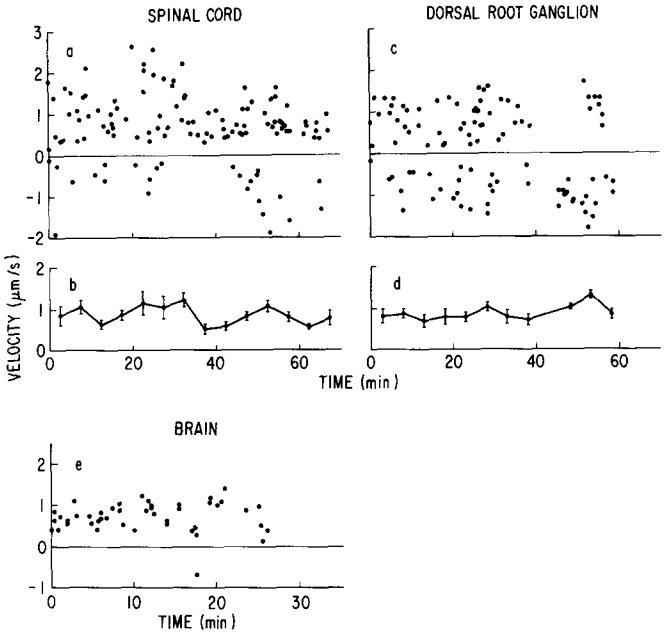

FIGURE 4 Translocation velocities of organelles in spinal cord (*a*), DRG (*c*), and brain cell (*e*) neurite bundles plotted vs. time illustrate the range of velocities of organelles. Positive and negative velocities refer to the direction of movement within the field, not in reference to the position of the soma. Means of scalar values of translocation velocities ± SD in spinal cord (*b*) and DRG cells (*d*) for all translocations occurring in 5-min increments demonstrate the constancy of this range of values over time.

make net progress in a given direction as indicated by high VSRs of 0.94 ± 0.04, 0.98 ± 0.01, and 0.95 ± 0.02 for spinal cord, DRG, and brain cells, respectively (Table III). In other words, while within a process a given organelle could be seen to reverse its direction of motion, nevertheless most organelles had a strong tendency to move in one direction. Further, in one small bundle of brain cell neurites (that shown by the arrows in Fig. 2) all but one of 45 organelles moved in a common direction (see Fig. 4 *e*).

Second, during any one translocation, each organelle demonstrated a wide frequency distribution of 1-s velocities (Fig. 6 *c*, *f*). In these distributions, determined for individual particles as shown in Figs. 5 and 6, discontinuities are probably attributable to the relatively low numbers of 1-s velocities. The composite frequency distribution of all the 1-s velocities of all analyzed organelles in a given cell type did not show such discontinuities. These composite frequency distributions (Fig. 5 *b*, *d*, *f*) were normalized so that each organelle's 1-s velocities would make the same percent contribution to the composite. This was done because slowly moving particles generated a greater number of 1-s velocities than did rapidly moving particles, and the normalization procedure prevented this fact from skewing the distribution toward the lower velocities. The normalization was done in the following way: for each particle, the percentage of time that it spent at each velocity was calculated (the procedure used in Fig. 6). This percentage time was then averaged over all particles to yield an average percentage time for that velocity; the range of all velocities was plotted as the composite frequency histogram of velocities (Fig. 5). Such composite frequency distributions of 1-s velocities of organelles in spinal cord, DRG, and brain cells are not exponential (i.e., are not linear on semilogarithmic coordinates), with spinal cord cells in particular having more high velocity movements than expected from an exponential distribution of velocities. Brain organelle 1-s velocities appear fairly equally represented in the 0–1.2 μm/s range with an abrupt drop in frequency of 1-s velocities greater than 1.4 μm/s (Fig. 5 *f*).

Third, large changes in 1-s velocity were frequently seen from second to second during the progress of any one organelle (Fig. 6 *b*, e). While some organelles were seen alternately to accelerate and decelerate from second to second, no uniform pattern of acceleration or deceleration in organelle behavior was noted.

Fourth, while it was sometimes observed that more than one organelle would slow down or stop at the same region along a neurite bundle, no bundles demonstrated common slow velocity zones for all, or even most, organelles. Two examples from brain cell cultures (Fig. 6 *b*, *e*) illustrate the variation of velocities manifested by organelles along the length of a neurite bundle. Plots of velocity vs. absolute distance along a neurite bundle for a number of organelle translocations revealed no common high or low velocity points.

Fibroblasts

Fibroblasts derived from dissociated mouse DRG cultures were examined after 5 days in culture (Fig. 1 *g*). Organelles within their broadened cytoplasmic extensions (Fig. 1 *h*) occasionally moved long distances at relatively high velocities,

TABLE III

Comparison of 1-s Velocities of Organelles in Different Types of Dissociated Cells in Culture

Cell type	No. of organelles analyzed	Mean vector velocity (μm/s) ± SD	Mean scalar velocity (μm/s) ± SD	Mean VSR
Spinal cord	21	1.1 ± 0.15	1.2 ± 0.15	0.94 ± 0.04
DRG	12	0.87 ± 0.10	0.88 ± 0.10	0.98 ± 0.01
Brain	25	0.69 ± 0.04	0.72 ± 0.04	0.95 ± 0.02
Fibroblast	6	0.07 ± 0.04	0.46 ± 0.09	0.12 ± 0.05
Neuroblastoma	5	0.11 ± 0.08	0.42 ± 0.08	0.19 ± 0.11

The VSR is an index of the net progress of an organelle in a given direction after several translocations as defined in the text (see Materials and Methods). Tabulated here are mean values of vector velocity, scalar velocity, and VSR for all organelles analyzed within a given cell type.

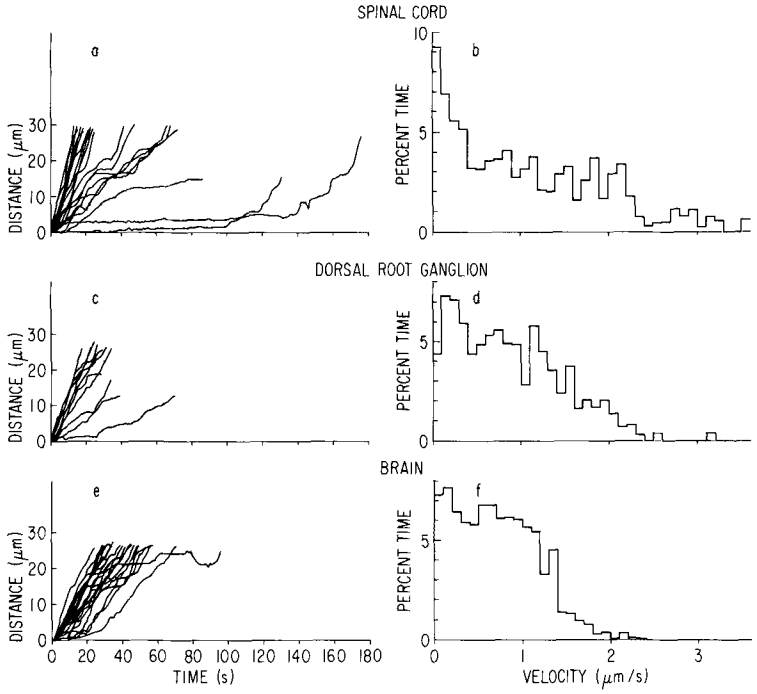

FIGURE 5 Behavior of organelles in neurite bundles of chick embryo spinal cord (*a*), chick embryo DRG (*c*), and rat embryo brain cells (*e*) as seen in these distance vs. time plots varies widely. Most, however, make significant net progress in a given direction. Initiation points of organelle trajectories, or the points in time at which moving organelles were noted to enter the frame, are all brought to the origin on the abscissa. Also, all organelle trajectories, regardless of whether they were seen to move from left to right or from right to left across the frame, are plotted in one direction, since in a neurite bundle one cannot distinguish proximal from distal motion. Fig. 5 *b*, *d*, and *f* are composite frequency distributions of all 1-s velocities of all organelle translocations analyzed in spinal cord (992 1-s velocities), DRG (382 1-s velocities), and brain cells (884 1-s velocities), respectively. Data from individual organelle translocations were normalized such that each translocation would make the same percent contribution to the composite, as described in Materials and Methods.

but most organelles moved slowly and were seen to hesitate and often reverse direction, manifesting a behavior markedly different from that of organelles in primary neuronal cultures (Fig. 7 *c*). The mean VSR of organelle translocation in fibroblasts was 0.12 ± 0.05 (Table II), reflecting the relatively low net progression of organelles in a given direction. As in primary neuronal cell cultures, any one organelle translocation was characterized by a wide distribution of 1-s velocities, and frequent and large changes in 1-s velocities from second to second were noted. Courses of long organelle translocations in fibroblasts were noted to be curved as well as straight, and often more than one particle traversed the same path. The composite frequency distribution of 766 1-s velocities of 12 organelles (Fig. 7 *d*) revealed a preponderance of slow velocities quite distinct from the frequency distribution of velocities in primary spinal cord, DRG, or brain cell cultures.

Continuous Cell Lines

Neuroblastoma, HeLa, and L cells were analyzed for organelle translocation. These cell types share the ability to produce processes either spontaneously or upon manipulation of their chemical environment. Approximately 100 cells from each of three clones of neuroblastoma prepared as described in Materials and Methods had similar organelle translocational behavior. Isolated processes of neuroblastoma cells were generally broader than those of isolated neurons in primary cultures, and contained greater numbers of larger organelles. The behavior of organelles was evalu-

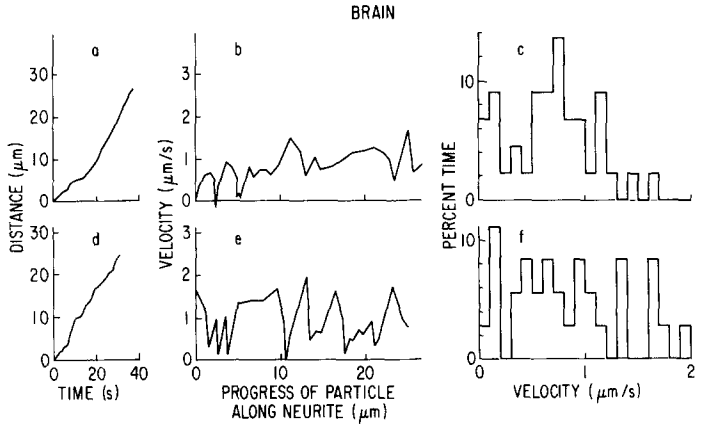

FIGURE 6 Second-by-second analysis of two organelles in rat embryo brain cells reveals that while portions of a given organelle's behavior seem to manifest relatively constant velocities in distance vs. time plots (*a*, *d*), frequent and marked percent changes in 1-s velocity are evident when the same data are plotted as velocity vs. absolute distance along a neurite bundle (*b*, *e*). Note that the organelles display widely divergent 1-s velocities at the same point in the neurite bundle. The discontinuities in the frequency distributions of 1-s velocities (*c*, *f*) are probably due to the low number of observations of each organelle.

ated in detail in the case of clone NX31, a sympathetic ganglion cell-neuroblastoma hybrid. As shown in Fig. 7 *a*, *b*, their behavior was similar to that described above for organelle movement in fibroblasts, and had a similarly low VSR.

HeLa cells, induced to form 40–60 μm long processes by the addition of 5 mM Na butyrate, were also studied. Organelles were seen to translocate in HeLa cells before and after butyrate treatment. L cells, induced to produce processes by the addition of 1 mM db-cAMP to the growth medium, revealed some translocational activity in their 20–30 μm long processes. Occasional organelle translocations were also noted in cells without processes and in the flattened perinuclear regions of cells with processes. In the processes of both treated HeLa and L cells, however, most translocations observed resulted in little net progress of a given organelle relative to that seen typifying organelle behavior in primary neuronal cultures.

Ultrastructural studies of similarly treated HeLa and L cells show the presence of some microtubules and numerous filaments about 100 Å in diameter in their processes. Microtubules in these cell processes, however, were neither so numerous nor so regularly arrayed as those in the DRG cell studied in detail.

DISCUSSION

The study of organelle motion, visualized by Nomarski optics and quantitated by computer, provides a direct approach to one type of axoplasmic flow. The range of organelle velocities observed in this study indicates that organelle motion may be responsible for some part of rapid axoplasmic flow, measured biochemically. The observed mean vector 1-s velocities (0.69–1.1 μm/s) are similar to the organelle velocities seen by others in neuronal systems (2, 17, 18, 26, 32, 33), including cerebellar neurons (12).[2] If an incorporated radioactive label were transported solely by the structures observed in this study, then maximal axoplasmic flow rates in our neuronal cells would be from 60 to 95 mm/day. This range is somewhat below the range generally reported for the fast component of transport (19) and between the slow and fast rates reported for chicken sciatic nerve (5). It may be that cultured neurons have slower rates of axoplasmic flow than neurons in vivo, and experiments are in progress to determine these rates in vitro. In addition, there are probably different classes of materials, moving at different rates (36), not all of which are visible with Nomarski optics. That particle motion underlies fast axoplasmic flow is also suggested by the depressant effect that metabolic inhibitors have on both processes (17), and the demonstration that fast axoplasmic flow consists primarily of particulate matter (5). Thus, it seems likely that some portion of fast transport is mediated by the motion

[2] David S. Forman, personal communication.

of particles visualizable by our methods. It should be pointed out that smaller, ill-defined structures near the limit of resolution of the light microscope can be seen apparently moving faster than any organelle analyzed in this report. Smaller structures, such as vesicles, seen in our electron micrographs, may also be moving.

Any mechanism of organelle motion must explain the features described in Table IV. The behavior of most particles in primary neuronal cells is quite different from the behavior of most

TABLE IV

Features of Organelle Motion

(*a*) Differences in velocities and VSRs between cell types.
(*b*) Linearity of most translocations.
(*c*) Motion in the absence of neurofilaments.
(*d*) Variation in translocational and 1-s velocities.
(*e*) The independence of velocity from location in neurite or from other organelles.
(*f*) High VSRs in primary neuronal cells.

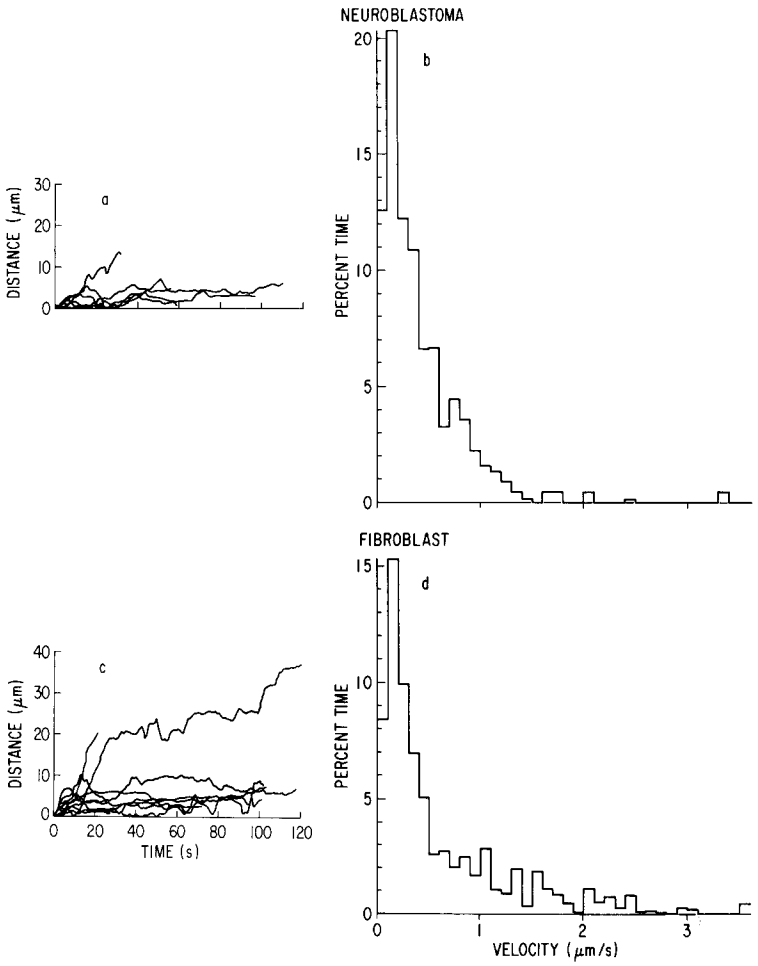

FIGURE 7 Behavior of organelles in isolated neuroblastoma hybrid NX31 cells (*a*) and DRG fibroblasts (*c*) as seen in these distance vs. time plots is strikingly different from that of primary neuronal cultures (Fig. 5). As in the equivalent plots in Fig. 5, initiation points of all organelle translocations are brought to the origin on the abscissa. Note the frequent reversals of direction and the failure of most organelles in both cell types to make significant net progress in one direction comparable to that in primary neuronal cultures. Note also the preponderance of slow 1-s velocities in the composite frequency distributions of 1-s velocities of organelle translocations in these cells. The latter are also quite distinct from frequency distributions of primary cultures (Fig. 5).

particles in fibroblasts or continuous cell lines observed in this study. The organelles of primary neuronal cultures (Fig. 5 *a*, *c*, *e*) have higher mean VSRs (Table III) than the organelles found in the broad cytoplasmic extensions of fibroblasts or processes of continuous cell lines (Fig. 7 *a*, *c*). Moreover, composite frequency distributions show that primary neuronal cells have a much higher probability of exhibiting fast 1-s velocities than the other cell types. The lack of sustained fast motion in the continuous cell lines examined may be due to a deficiency in either the genotype or the degree of differentiation attained in our culture system. Although the ultrastructural and biochemical correlates of these differences have yet to be determined, the presence of microtubules in L cells suggests that microtubules alone are not a sufficient condition for the rapid, organized transport seen in primary neuronal cells. However, the observations suggest a relationship between characteristics of organelle translocation and the density and orderliness of microtubule packing. Thus, in L cells, organelle movement has a low VSR and microtubules are generally found at lower densities and in less orderly arrays than in the neurites of primary neuronal cells, which have high VSRs.

Long linear subcellular structures such as microtubules, microfilaments, or the axolemma have been proposed to account for the guidance or propulsion of organelles (20, 23, 28). The trajectories of moving particles in HeLa cells have been shown to correspond to the orientation of microtubules (14). The case for the microtubule mediation of organelle transport has been strengthened by the demonstration that in neurons microtubules are associated with mitochondria (27, 31, 33, 34, 37) and synaptic vesicles (16, 30). Because electron micrographs from these works show more than one microtubule associated with a mitochondrion, perhaps microtubules cooperate in organelle translocation. In addition, drugs such as colchicine, vinblastine, and podophyllin, which bind to and impair the structure of microtubules, generally block organelle translocation (3, 13, 14) although some rapid axonal transport has been reported after large reductions in the number of microtubules (6). The DRG neurite of the present study had plentiful microtubules but neither 100-Å neurofilaments nor other linearly oriented microfilaments. Organelle saltations in the presence of colchicine have been reported (1, 9), but in no case was the absence of microtubules shown by electron microscopy. Organelle translocation and the transport of label in the presence of microtubules and absence of microfilaments have also been seen in heliozoan axopodia (35) and the crayfish nerve cord (10). Therefore, although the involvement of microtubules has not been conclusively demonstrated, it would appear that substantial numbers of linear microfilaments and 100-Å neurofilaments are not necessary for transport in some cells.

Organelle motion was also shown to be discontinuous, involving a number of translocations of varying lengths and velocities. Moreover, during one translocation, an organelle's 1-s velocity varied widely. Generally, such behavior can be explained either by changes in the local resistance to forward motion or by changes in motive force. In the former case, variations in cytoplasmic viscosity or the presence of subcellular structures might hinder the displacement of organelles. However, when the velocities of many organelles, plotted as a function of distance along a neurite, were compared, no common high or low velocity zones were seen. This was true in the DRG process shown by electron microscopy to be a single neurite, and in the small brain fascicle having one or a few neurites. Therefore, if zones of high or low resistance exist, they do not extend uniformly across a neurite or bundle of neurites. We cannot rule out discrete changes in the resistance in various "channels" that organelles may follow through the cytoplasm.

Variations in motive force could be due to discontinuities or irregularities in linear subcellular structures such as microtubules, or to local variations in the concentrations of possibly required substances such as ATP or divalent cations. Again, because no common points of high or low velocity were seen when many particles in the same neurite were analyzed, variations of force can only explain the data if particles are transported along various channels in any one neurite, and thus are not equally affected by regional changes in motive force within one channel. In any case, the temporal variations in organelle velocities are not due to the organelles passing through standing longitudinal gradients of resistance or motive force common to the entire neurite.

Variation in organelle velocities could also be due to the random association and dissociation of an organelle with one or more linearly oriented structures. According to this model, at any instant each associated linear structure would contribute some amount of propulsive force to the organelle,

but the number of associated linear structures would vary randomly with time. Assuming a uniform number of linear structures along the length of a process, such a model implies the observed discontinuities of an organelle's velocity, without implying the existence of fixed zones where all organelles would exhibit maximal or minimal velocities. In addition to explaining the independence of an organelle's velocity from its position along the axon, this model also explains why its motion is usually dissociated from the motion of other organelles in the neurite.

Whatever the mechanism of organelle translocation, it must also account for the high VSRs observed in the present study. Although different organelles in the same neurite were observed to have opposite directions of net translocation, and although the same organelle often stopped and occasionally reversed direction, the net progress of an individual organelle, as quantified by its VSR, was extremely high in primary neuronal cells (Table III). This implies that, although a neurite is capable of transporting organelles in both directions, some component of the system has a directional valence which preserves the direction of an organelle's motion during great changes in its velocity. We also wish to raise the possibility that, in primary neuronal cells, each organelle has a code and that some structure must recognize and direct the motion of that organelle in either a proximal or distal direction.

The authors wish to acknowledge the expert technical assistance of Ms. Marie Neal and Ms. Mary Lou Adams, and the advice of Mr. William Sheriff and Dr. James Dvorak. The continuous cell lines were generous gifts from Drs. Xandra Breakefield, Hayden Coon, Lloyd Greene, John Minna, Marshall Nirenberg, and William Shain.

After this manuscript was submitted for publication, there appeared in print: Cooper, P. D., and R. S. Smith. 1974. The movement of optically detectable organelles in myelinated axons of *Xenopus laevis*. *J. Physiol. (Lond.)*. **242**:77–97.

Dr. C. N. Christian is the recipient of National Institute of Child Health and Human Development postdoctoral fellowship 5-F02-HD55299-02.

Received for publication 14 November 1974, and in revised form 12 February 1975.

BIBLIOGRAPHY

1. ALLEN, R. D. 1974. Some new insights concerning cytoplasmic transport. *Symp. Soc. Exp. Biol.* **28**:15–26.
2. BERLINROOD, M., S. M. MCGEE-RUSSELL, and R. D. ALLEN. 1972. Patterns of particle movement in nerve fibers *in vitro*: An analysis by photokymography and microscopy. *J. Cell Sci.* **11**:875–886.
3. BICKLE, D., L. G. TILNEY, and K. R. PORTER. 1966. Microtubules and pigment migration in the melanophores of *Fundulus heteroclitus L. Protoplasma.* **61**:322–345.
4. BORNSTEIN, M. B. 1958. Reconstituted rat-tail collagen used as a substrate for tissue cultures on coverslips in Maximow slides and roller tubes. *Lab. Invest.* **7**:134–137.
5. BRAY, J. J., and L. AUSTIN. 1969. Axoplasmic transport of ^{14}C-proteins at two rates in chicken sciatic nerve. *Brain Res.* **12**:230–233.
6. BYERS, M. R. 1974. Structural correlates of rapid axonal transport: evidence that microtubules may not be directly involved. *Brain Res.* **75**:97–113.
7. DAHLSTROM, A. 1967. The intraneuronal distribution of noradrenalin and the transport and life-span of amino storage granules in the sympathetic adrenergic neuron. *Naunyn-Schmiedebergs Arch. Exp. Pathol. Pharmakol.* **257**:93–115.
8. DVORAK, J. A., and W. F. STOTLER. 1971. A controlled environment culture system for high resolution light microscopy. *Exp. Cell Res.* **68**:114–148.
9. EDDS, K. 1973. Particle movements in artificial axopodia of *Echinosphaerium nucleofilum*. *J. Cell Biol.* **59**(2, pt. 2): 88 a. (Abstr.).
10. FERNANDEZ, H. L., P. R. BURTON, and F. E. SAMSON. 1971. Axoplasmic transport in the crayfish nerve cord. The role of fibrillar constituents of neurons. *J. Cell Biol.* **51**:176–192.
11. FISCHBACH, G. D. 1972. Synapse formation between dissociated nerve and muscle cells in low density cell cultures. *Dev. Biol.* **28**:407–429.
12. FORMAN, D. S., G. R. SIGGINS, and R. S. LASHER. 1973. Rapid intracellular movements of particles in cultured cerebellar neurons. Society for Neuroscience Program and Abstracts, Third Annual Meeting. Society for Neuroscience, Bethesda, Md. 146.
13. FREED, J. J., A. N. BHISEY, and M. M. LEBOWITZ. 1968. Patterns of movement in cultured cells treated with agents affecting microtubules. *J. Cell Biol.* **39** (2, Pt. 2):148 a. (Abstr.).
14. FREED, J. J., and M. M. LEBOWITZ. 1970. The association of a class of saltatory movements with microtubules in cultured cells. *J. Cell Biol.* **45**:334–354.
15. GINSBURG, E., D. SALOMON, T. SREEVALSAN, and E. FREESE. 1973. Growth inhibition and morphological changes caused by lipophilic acids in mammalian cells. *Proc. Natl. Acad. Sci. U. S. A.* **70**:2457–2461.
16. JARLFORS, U., and D. S. SMITH. 1969. Association between synaptic vesicles and neurotubules. *Nature (Lond.)*. **224**:710–711.
17. KIRKPATRICK, J. B., J. J. BRAY, and S. M. PALMER. 1972. Visualization of axoplasmic flow *in vitro* by Nomarski microscopy. Comparison to rapid flow of radioactive proteins. *Brain Res.* **43**:1–10.

18. KIRKPATRICK, J. B., and L. Z. STERN. 1973. Axoplasmic flow in human sural nerve. *Arch. Neurol.* **28**:308–312.
19. LASEK, R. J. 1968. Axoplasmic transport in cat dorsal unit ganglion cells: As studied with ^{3}H-L-leucine. *Brain Res.* **7**:360–377.
20. LASEK, R. J. 1970. Protein transport in neurons. *Int. Rev. Neurobiol.* **13**:289–324.
21. LEVI-MONTALCINI, R., and P. U. ANGELETTI. 1963. Essential role of the nerve growth factor in the survival and maintenance of the dissociated sensory and sympathetic embryonic nerve cells *in vitro*. *Dev. Biol.* **7**:653–659.
22. LUBINSKA, L. 1964. Axoplasmic streaming in regenerating and in normal nerve fibers. *Prog. Brain Res.* **13**:1–66.
23. MCCLURE, W. O. 1972. Effect of drugs upon axoplasmic transport. *Adv. Pharmacol. Chemother.* **10**:185–220.
24. NELSON, P. G., and J. H. PEACOCK. 1973. Transmission of an active electrical response between fibroblasts (L-cells) in cell culture. *J. Gen. Physiol.* **62**:25–36.
25. OCHS, S., and J. JOHNSON. 1969. Fast and slow phases of axoplasmic flow in ventral root nerve fibers. *J. Neurochem.* **16**:845–853.
26. POMERAT, C. M., W. J. HENDLEMAN, C. W. RAIBORN, JR., and J. F. MASSEY. 1967. Dynamic activities of nervous tissues *in vitro*. *In* The Neuron. H. Hyden, editor. American Elsevier Publishing Co. Inc., New York. 119–178.
27. RAINE, C. S., B. GHETTI, and M. L. SHELANSKI. 1971. On the association between microtubules and mitochondria within axons. *Brain Res.* **34**:389–393.
28. REBHUN, L. I. 1972. Polarized intracellular particle transport: Saltatory movements and cytoplasmic streaming. *Int. Rev. Cytol.* **32**:93–137.
29. SEEDS, N. W., A. G. GILMAN, T. AMANO, and M. NIRENBERG. 1970. Regulation of axon formation by clonal lines of neural tumor. *Proc. Natl. Acad. Sci. U. S. A.* **66**:160–167.
30. SMITH, D. S., U. JARLFORS, and R. BERANEK. 1970. The organization of synaptic axoplasm in the lamprey (*Petromyzon marinus*) central nervous system. *J. Cell Biol.* **46**:199–219.
31. SMITH, D. S., U. JARLFORS, and B. F. CAMERON. 1974. Morphological evidence for the participation of microtubules in axonal transport. The New York Academy of Sciences Conference on the Biology of Microtubules, Abstracts. New York Academy of Sciences, New York, 26.
32. SMITH, R. S. 1971. Centripetal movement of particles in myelinated axons. *Cytobios.* **3**:259–262.
33. SMITH, R. S. 1972. Detection of organelles in myelinated nerve fibers by dark-field microscopy. *Can. J. Physiol. Pharmacol.* **50**:467–469.
34. SMITH, R. S. 1973. Microtubule and neurofilament densities in amphibian spinal root nerve fibers: Relationship to axoplasmic transport. *Can. J. Physiol. Pharmacol.* **51**:798–805.
35. TILNEY, L. G. 1971. Origin and continuity of microtubules. *In* Origin and Continuity of Organelles. J. Reinert and H. Ursprung, editors. Springer-Verlag, Berlin. 222–260.
36. WILLARD, M., W. M. COWAN, and P. R. VAGELOS. 1974. The polypeptide composition of intra-axonally transported proteins: evidence for four transport velocities. *Proc. Natl. Acad. Sci. U. S. A.* **71**:2183–2187.
37. WUERKER, R. B., and J. B. KIRKPATRICK. 1972. Neuronal microtubules, neurofilaments, and microfilaments. *Int. Rev. Cytol.* **33**:45–75.